NASA TECHNICAL MEMORANDUM

NASA TM-73822

NASA TM-73822

(NASA-TM-73822) RELEASE OF DISSOLVED NITROGEN FROM WATER DURING DEPRESSURIZATION (NASA) 20 p HC A02/MF A01 CSCL 07D

N78-17172

Unclas
G3/25 04475

RELEASE OF DISSOLVED NITROGEN FROM WATER DURING DEPRESSURIZATION

by R. J. Simoneau
Lewis Research Center
Cleveland, Ohio 44135

TECHNICAL PAPER to be presented at the
Fourteenth Annual Meeting of the
Southeastern Seminar on Thermal Sciences
Raleigh, North Carolina, April 6-7, 1978

E-1411-1

RELEASE OF DISSOLVED NITROGEN FROM WATER DURING DEPRESSURIZATION*

R. J. Simoneau
National Aeronautics and Space Administration
Lewis Research Center
Cleveland, Ohio 44135

ABSTRACT

Experiments were run to study depressurization of water containing various concentrations of dissolved nitrogen gas, the primary case being room temperature water saturated with nitrogen at 4 MPa. In a static depressurization experiment, water with very high nitrogen content was depressurized at rates from 0.09 to 0.50 MPa per second and photographed with high speed movies. The pictures showed that the bubble population at a given pressure increased strongly with decreasing depressurization rate. Bubbles rarely appeared before the pressure reached $P_o/2$. Flow experiments were performed in an axisymmetric converging-diverging nozzle and in a two-dimensional converging nozzle with glass sidewalls. Depressurization gradients were roughly 0.5×10^3 to 1.2×10^3 MPa per second. Both nozzles exhibited choked flow behavior even at nitrogen concentration levels as low as 4 percent of saturated. The flow rates were independent of concentration level and could be computed as incompressible water flow based on the difference between stagnation and throat pressures; however, the throat pressures were significantly different between the two nozzles.

NOMENCLATURE

C_D discharge coefficient, dimensionless

C_{N_2} nitrogen concentration in the water referenced to 1 atmosphere pressure and 25 C, cc/g

G flow rate, g/cm^2-sec

P pressure, MPa

T temperature, K

t time, sec

ρ density, g/cm^3

---

*Some of this material was previously presented in a report to the U.S. Nuclear Regulatory Commission, November 1977.

Subscripts:

max maximum

o stagnation conditions in flow experiments - initial pool conditions in static depressurization experiments

t throat conditions

INTRODUCTION

Many liquids contain a sizable quantity of gases dissolved under pressure. Soft drinks and champagne are common examples. Of more current technical significance, the emergency core cooling water in a pressurized water reactor system is stored under nitrogen pressure. During storage the nitrogen will slowly dissolve into the water and in time we can expect the ECCS water to be fully saturated with nitrogen at the storage temperature and pressure. The question of technical interest then is what happens to the nitrogen should the system be called to action and the nitrogen laden water start depressurizing while flowing into the main flow loop to the core.

Published solubility data [1] show, for instance, that 1 gram of water at room temperature and 4.24 MPa pressure can contain up to 0.62 cc of nitrogen measured at room temperature and 1 atmosphere. (Note: At atmospheric pressure 1 gram of saturated water contains only 0.015 cc of nitrogen.) This much nitrogen could produce a void fraction of 38 percent during depressurization of fully saturated water from 4.24 to 0.1 MPa (600 to 0 psig).

A study is underway at NASA Lewis Research Center to examine the bubble size and rate of nitrogen bubble evolution and its effect on flow during depressurization transients. This study is being conducted in two ways, both with an emphasis on visual and pressure history information. First, a static (more accurately nonflow) depressurization test was conducted in a small, 5-liter vessel with viewing ports to observe the water during the depressurization transient. Second, a steady flow of nitrogen saturated water was discharged through a nozzle pressure gradient while pressure, flow rate, and visual data were recorded. This paper contains the preliminary results of these two experiments.

TEST APPARATUS

Static Depressurization Rig

The static depressurization rig was a nonflow system in which the nitrogen saturated water could be depressurized at a controlled rate and observed visually. It is shown schematically in figure 1. The two major components were a 30-liter high pressure storage vessel and a 5-liter high pressure viewing vessel. The system could be operated up to 4.0 MPa. Nitrogen was dissolved into the water, while in the storage tank, by bubbling nitrogen gas through the vessel from the bottom under pressure. The flow was controlled by a metering needle valve and the pressure controlled by a back-pressure regulator. The flow rate was set at a level to assure a continuous flow-through of gas. After some desired bubbling time the water containing dissolved nitrogen was transferred to the viewing vessel using a small pressure differential, on the order of 0.07 MPa or less. During the transfer the water passed through a removable bottle of approximately 12 cc capacity. This allowed drawing a high pressure sample for nitrogen content analysis.

Internally the viewing vessel was approximately 15 cm in diameter and 29 cm high. The measured volume, including the window penetrations, was close to 5.0 liters. The viewing window was 6.5 cm in diameter and was located approximately three-fourths of the distance from the bottom. The pool was illuminated through a similar window in the top of the vessel. The internal components are shown in figure 2. The wire mesh cylinder was used to promote gas nucleation sites. The probe to the far right was a Chromel-Constantan thermocouple. The L-shaped probe was used to mark liquid level. The pointed tip was located at the 90 percent full level. The ladder shaped device was used for dimensional reference. The rungs alternated in diameter, with the top one being 0.25 mm and the next one 0.51 mm and so on down. They were spaced 0.50 cm apart.

Flow Rig

The flow rig was a modification of a facility used extensively for experiments in two-phase choked flow of subcooled cryogens [2]. A schematic of the essential features is shown in figure 3. The main flow setup consisted of a 110-liter pressure vessel capable of pressures up to 10 MPa; an orifice flowmeter; the test section; a back pressure control valve; and a weigh tank. Nitrogen gas was bubbled in through the bottom of the tank and controlled with a back pressure regulator. During flow nitrogen gas pressure was maintained on the top of the vessel from a high pressure bottle farm. Because the main tank was small, a 375-liter storage vessel, in which additional water could be saturated with nitrogen gas, was added to the system.

The test sections used in the present experiment are shown in figures 4 and 5. Figure 4 shows a conical axisymmetric converging-diverging nozzle used extensively in the cryogenic experiments [2]. Nine of the 15 pressure taps were used in the present experiment. The throat region had a constant area section which was 3.2 diameters long. Figure 5 shows a visual test section which was designed for use in this experiment. It was made by taking a conventional commercial high pressure sight gage and replacing the centerbody with the one illustrated in figure 5. In addition to its visual characteristics the essential features of this test section were the linear converging pressure gradient and the abrupt area change at the exit of the minimum area region. The minimum area or "throat" region had a length of constant cross-sectional area which was one channel height long. The gasket sealing the glass sidewalls to the centerbody was trimmed slightly to achieve a better view of the edge. This gave the throat region a slight I-shape. There were nine pressure taps located axially along the nozzle as shown in figure 5.

Instrumentation

Pressures throughout were measured with strain gage transducers. The pressure lines were not bled. Temperatures at the inlet and outlet of the flow test sections were measured with platinum resistance thermometers. In the flow rig the mass flow rate was measured with a calibrated orifice just upstream of the test section, and was checked by weighing the flow discharge.

The photographic data records were obtained by use of movies. In the static depressurization facility two cameras were used simultaneously, one running at real time (24 pictures per second, pps) and one running at 200 or 400 pps depending on the rate of the transient. The light was 90° to the viewing port. As the transient progressed the bubble population significantly changed the lighting. Both cameras were equipped with automatic exposure controls. In the flow facility the pictures were taken with a high speed camera operating at 9000 pps and an exposure time of 1/27,000 of a second. The lighting was from the rear through the test section.

Gas Content Analysis

The nitrogen content of the water was determined as follows. First, the high pressure sample in the 12 cc bottle was discharged into a known volume which had been evacuated. The chambers were sized so that the final equilibrium pressure would be near atmospheric pressure. The volume of nitrogen discharged was computed from the final pressure by the ideal gas law. A correction was made for the partial pressure of the water vapor. The sample was then sent to the chemical analysis laboratory to measure the residual nitrogen content. The final result was expressed as the number of cubic centimeters of nitrogen measured at 25° C and 1 atmosphere contained in 1 gram of water (cc/gm).

RESULTS

Time Scale of the Experiments

The two experiments had significantly different time scales. In the static depressurization experiment the average depressurization rates ranged from about 0.1 to 0.5 MPa per second. In the flow tests the combination of steep pressure gradients and short residence times produced average depressurization rates on the order of 0.5×10^3 to 1.2×10^3 MPa per second. This three order of magnitude greater rate is more in line with the rate one might expect in a typical emergency core cooling system (ECCS) of a pressurized water reactor (PWR). Typically, the ECCS water, presumably saturated with nitrogen, discharges through about 8 meters of 23 cm pipe before joining the large 76 cm diameter cold leg pipe. A rough estimate of the maximum depressurization rate in this pipe is 7.0×10^3 MPa per second.

We can see that we should look more to the flow data to make a realistic interpretation of the nitrogen release phenomena. On the other hand, because of the very short time scale, it was very difficult to obtain detailed mechanism information from the flow tests. The static depressurization tests were useful in qualitatively evaluating the variables.

Static Depressurization Results

The static depressurization tests reported herein were all conducted with distilled water at room temperature (approximately 22° C) and an initial pool pressure of 3.86 MPa. A parametric array of gas bubbling times (i.e., gas concentrations) and depressurization rates were examined. The depressurization rates were nonlinear (nearly exponential) and are reported herein as the time it took the system to depressurize to $P_o/3$. (The average rate in this process is approximately $-2P_o/3t$.) This time to $P_o/3$ ranged from 5 to 30 seconds in these tests. Nitrogen gas was bubbled through the water prior to depressurization for six different periods ranging from 1 to 28 days.

It was clear from the gas content measurements that it was not necessary to bubble the nitrogen through the water for such long periods to achieve high concentration values. Bubbling times of 3 to 6 days seemed more than adequate to bring the water to very large, near-saturated gas content levels.

On the other hand, as one might expect, there was a general trend of increased gas content with increased bubbling time. For example, after 12 days bubbling the nitrogen content was measured to be 0.57 cc/gm and at 28 days it was 0.61 cc/gm. Unfortunately, the data scatter in the gas concentration measurements was comparable to this 7 percent trend. Since the measurements for both bubbling times were at or above the published saturation value of 0.57 cc/gm, it was felt that the 28 day soak represented a fully saturated pool of water.

In addition to the nitrogen content, the variable of main interest is the rate of depressurization of the pool of water which has been saturated with nitrogen gas. As explained above this was expressed in terms of the time to depressurize to $P_o/3$. In figures 6 and 7 single frames from the depressurization movies are arranged in arrays to show the influence of depressurization times on bubble population. Figure 6 shows the results for room temperature water saturated with nitrogen at 0.61 cc/gm (28 day bubbling time) which was depressurized from an initial pressure of

3.86 MPa. The figure shows the bubble population at five pressure levels during transients at four different times to depressurize to $P_o/3$. Figure 7 is an identical array of photographs for water with a nitrogen concentration of 0.57 cc/gm (12 day bubbling time), which is 93 percent of the maximum average value.

It is clear from both figures that the influence on bubble population of the time to depressurize to $P_o/3$ is strong, especially if the water is not fully saturated with gas. The general trend, that bubble population increases as depressurization rate decreases, is obvious. It should be noted that in both figures the pressure in the first row is already down to $P_o/2$. Thus we can see that, even though the water was saturated or nearly saturated with nitrogen at P_o, there is very little bubble evolution when the pressure has dropped to half of its original value. By this time the water is highly supersaturated with nitrogen. Recall that these depressurization rates are very slow by reactor standards. When the bubbles do begin to come out they do not explode out as can be seen by the depressurization sequences.

If the nitrogen content is somewhat less than saturated (fig. 7) the delay in initial bubble evolution is fairly strong. Of course, since the total nitrogen content is only slightly lower, the final bubble populations will be similar (see both figures at $P_o/10$).

The majority of the bubbles which appear in figures 6 and 7 are fully matured in growth for that pressure level. They were formed in the lower half of the vessel and rose into view. They are quite small ranging from about 0.1 to 1.0 mm in diameter with the vast majority more uniformly grouped around 0.2 to 0.5 mm. These estimates are based on comparisons with the reference wire diameters on the ladder shaped device (c.f., fig. 2). At lower pressures, $P/P_o = 0.1$ for instance, it was very difficult to see because of high population; however, some large bubbles of 2 to 3 mm size did appear but they were a small percentage of the whole. Generally the bubbles in view were roughly the same size independent of the pressure level. Since the bubbles are rising past the window, the time between being formed and being seen and the associated pressure differential should be roughly constant. This suggests that the bubble forms at about the same size independent of the water pressure. Thus at the end of the transient there should be a spectrum of bubble sizes with the bubbles formed early at high pressure having grown large and the newly formed bubbles remaining small. There was very little, almost no, bubble coalescence even at low pressure when the bubble population was very high. The only place where some would coalesce was at stagnation points, such as the window rim.

Some data were taken to assess the influence of settling time between transfer of the water from the storage to the viewing tank and the depressurization transient. For the data discussed so far this was normally 15 to 30 minutes with a few being 1 to 2 hours. For each bubbling period, however, one set of data were taken where the viewing pool was allowed to sit overnight, approximately 20 hours, after transfer and before depressurization. During this time bubbles would begin to diffuse out of solution and attach to the surfaces, including the windows, much like a glass of tap water that has been allowed to sit for some time. The depressurization transients were always at the slowest rate, 30 sec to $P_o/3$. Bubbles formed much earlier in the transient but not in great quantity. By the time the pressure was down to $P_o/3$, for example, there seemed to be little difference in the bubble density compared to the short settling time runs. It seems these prematurely formed bubbles had only small influence on the overall bubble population.

Flow Through Nozzle Results

Data were acquired for the conical axisymmetric converging-diverging stainless steel nozzle (fig. 4) and the two-dimensional converging visual nozzle (fig. 5). The water was deionized tap water.

The pressure distributions through the converging-diverging nozzle for three different concentrations of N_2 are shown in figure 8. Figure 8 has each of the three sets of data shifted slightly on the ordinate so that they can be seen distinctly. The highest concentration level, 0.62 cc/g, represents water fully saturated with nitrogen at the stagnation pressure, 4.18 MPa. Another is at half that concentration, 0.31 cc/g, which is equivalent to saturating the water at 2.2 MPa. No nitrogen was added to the final set. The water as drawn from the tap through the deionizer was found to contain 2 to 2.5 percent by volume dissolved nitrogen. All other significant parameters were nominally constant.

All of the data in figure 8 meet the classic criteria for choking. A significant change in back pressure (up to 1 MPa) produces no change in flow rate or throat pressure. This condition exists for all three sets of data in figure 8. Furthermore, the pressure profiles are absolutely identical for all three concentration levels. If the fluid is not compressible, one is at a loss to explain the ability to significantly raise the back pressure without reducing the flow. In one case (not shown) the back pressure was raised to $P_o/2$ with no effect. It would appear that water containing dissolved nitrogen can choke and that the choking flow rate and pressure profiles are independent of the nitrogen concentration level. It is possible that the fluid pressure at the throat was so low as to flash to vapor. However, at these temperatures this would be a very low pressure, 0.002 to 0.003 MPa.*

The flow rate results are shown in figure 9. The independence of flow rate from nitrogen concentration level is obvious. In figure 9 the choked

*It should be noted that the actual throat pressure readings of 0.02 to 0.05 MPa are beyond the accuracy of the 6.90 MPa (1000 psig) transducers. Thus, the numbers can only be reported as very low, and the throat pressures could be as low as 0.002 to 0.003 MPa, thereby permitting vaporization.

flow rates are compared to those computed by discharging incompressible water with $(P_o - P_t) \approx P_o$.

$$G_{max} \approx C_D \sqrt{2\rho P_o}$$

The nozzle was calibrated in a flow calibration laboratory and the asymptotic C_D was found to be 0.946. The agreement between the maximum flow rates and the above approximation is excellent. Thus although the flow was choked the flow rate can still be computed in the above situation by treating it as a discharge of all liquid into a 1-atmosphere reservoir. This is consistent with the results of Henry and Cha [3], who found little difference in blowdown times whether the water was saturated or not. This result, however, should be treated as highly empirical and applicable only to situations comparable to the one above. The above equation should apply if the minimum flow areas occur early in the flow passage; if the depressurization gradient to the minimum flow area is quite steep; and, particularly, if the minimum area is substantially smaller than any other cross-section.

The data taken in the two-dimensional visual nozzle present a more complex picture. The physical constraints of the visible channel made it necessary to provide fairly small entrance and exit passages to the test section. The flow area in these passages was only on the order of 2.5 times the minimum (throat) area of the nozzle. The small passage at the entrance caused a large pressure drop between the tank and the test section (approx. 1.0 MPa at the 4.2 MPa level). Thus the fluid pressure entering the test section was already 25 percent below saturation. At no time did any bubbles appear in this test section entrance region.

The pressure profiles in the visual nozzle are displayed in figure 10 in the same manner as those for the C-D nozzle in figure 8. In general, the same remarks and conclusions apply here. The flow acts choked. Significant back pressure changes can be made with no upstream effect. The profiles and flow rates seem independent of nitrogen concentration. However, some significant differences exist. First, the "throat" pressures are approximately an order of magnitude higher, and they are a little bit different from run to run (0.53 MPa in the C_{N_2} = 0.02 cc/gm case and 0.65 MPa in the saturated case). Second, a liquid core jets into the abrupt area change region downstream of the "throat." Third, the flow downstream of the "throat" is clearly not one-dimensional. These later two effects can be seen in the movies of the flow.

Figure 11 shows prints of selected frames of movie photographs of the flow discharging through this nozzle taken at about 9000 pictures per second (pps). The liquid jets are seen beyond the throat, in the expansion region, and gas begins to appear along the edges of the jet (fig. 11(b)). Thus, in this case with the abrupt area change, it may be incorrect to interpret the pressure measured at the nozzle "throat" as being related to the pressure of nitrogen release. This is in contrast to the C-D nozzle where the nitrogen is assumed to be released at the throat. The jet sometimes attached to the right wall and sometimes to the left (more often to the left). In any given run it did not bounce back and forth. It chose a wall and stayed there. The point of attachment did oscillate slightly axially but was roughly at the second downstream pressure tap. The pressure taps were on the left. Notice in figure 10 usually the first pressure downstream of the throat is quite a bit lower, then jumps to a very high value and starts dropping off again - all in a constant area region. This would be consistent with the jet impacting the second tap. In one case in figure 10 the downstream pressures were virtually constant. In that run it was observed visually that the jet attached to the right side, opposite the pressure taps. Although it is obvious the flow is highly two-dimensional downstream, it is not clear what this says about the nitrogen release pressure, since all the pressures measured are quite high relative to the C-D nozzle. Figure 11 makes it very clear, however, that gas is coming out of solution. The overall pressure level is two orders above the vaporization pressure. The amount of gas produced appears to be proportional to the concentration of dissolved nitrogen in the water.

The choking in this case could be occurring in the exit passage of the test section which is about 2.5 times the flow area of the "throat." That the flow is choked is clear from the large variation in back pressure having no effect on the flow rate or pressure distribution (c.f., fig. 10). The data do not necessarily indicate the point of choking. Thus, it is possible to drop the pressure low enough at one constriction to cause nitrogen release and then have choking occur somewhere else downstream at a somewhat larger constriction. In the steady-state case the distinction of the location of choking is merely a fine point in the study, since the flow can be computed on the basis of that first pressure drop. In the transient blowdown case the consequences are not so clear. The flow rates based on

$$G = \sqrt{2\rho(P_o - P_t)}$$

for the two cases in figures 1(a) and (b) (c.f., fig. 10) are 7160 and 7350 g/cm^2 second, respectively, which are in good agreement with the data. The flow rate data from both nozzles support the conclusion that the flow can be computed as an incompressible all liquid flow based on the pressure drop from stagnation region to the nozzle throat. Unfortunately, the two nozzles also offer no guidance as to what this "throat" pressure will be.

Nucleation

These experiments do not yield details on the gas nucleation mechanisms; however, some general remarks can be made from the results of the two experiments. While it is not obvious from a single frame such as in figures 6 and 7, the static depressurization movies indicate that the bubbles originated from the metal surfaces especially the cylindrical screen. The bubbles maintain a cylindrical pattern as they rise in the pool. From some of the frames of figures 6 and 7 it appears that bubbles are also originating on the ladder shaped device and on the walls. Frequently in the depressurization transient just before identifiable bubbles would appear the window would get cloudy, like a film forming on the window. It is not clear whether this was related to nucleation since bubbles never grew from the windows but it did seem to signal a change.

Similarly, in the flow experiments the bubbles appear to be nucleating from the edge of the nozzle throat walls (fig. 11(b)). Again, watching the movies is much more informative than viewing a single frame. Unfortunately, even at 9000 pps the action could not be adequately stopped to identify individual bubbles.

The literature is not very helpful in this area. Most of the work on dissolved gases has focused on the influence of the gas on vaporization of the liquid and generally the concentrations are low [4-6]. Solutions for bubble growth rate which cover a wide concentration range, such as the work of Epstein and Plesset [7], assume the gas concentration stays constant relative to saturation which is not the case in the depressurization experiment. The equations will have to be reformulated to include the growth rate due to pressure change as well as diffusion. This in turn will require a way of estimating the initial gas volume of the nuclei. The present experiments offer only end point checks on these eventual calculations. The analysis will also have to agree with the fact that in the flow experiments the nozzle throat pressure was independent of gas concentration.

SUMMARY AND CONCLUSIONS

The experiment had two major components: a static depressurization experiment and a flow through a pressure gradient experiment. In the static depressurization experiment nitrogen was dissolved into water by bubbling the gas through under high pressure, 3.85 MPa, for a period of from 1 to 28 days. The nitrogen laden water was then depressurized at rates ranging from 0.09 to 0.50 MPa/second and the transient was recorded using high speed movies. In the flow experiments the water containing dissolved nitrogen was flowed through various nozzles. Flow rates, pressure profiles and high speed movies were recorded. Pressure changes were in the order of 0.5×10^3 to 1.2×10^3 MPa/second, about three orders greater than the static tests and more realistic in terms of potential application of the results.

The static (or nonflow) test results, despite a relatively slow transient yield some interesting information on the process. Starting from the same initial pressure, it can generally be said that at any given pressure level in the transient there will be more bubbles present the lower the depressurization rate and the longer the bubbling time. The rate effect over the range investigated is fairly strong. At the highest rate, 0.50 MPa/second, it was possible in some cases to reach $P/P_o = 0.20$ without the appearance of any bubbles, while the slowest rate, 0.09 MPa/second, bubbles were routinely present at $P/P_o = 0.30$. Although the concentration measurements did show fairly short times to near saturation, it was possible to continue to add small quantities of dissolved gas to the water by bubbling over long periods. If the nitrogen concentration was slightly below saturation, the initial bubble evolution pressure was substantially lower.

The static tests also yielded some detail on bubble size. In general the mature nitrogen bubbles are quite small, on the order of 0.1 to 1.0 mm in diameter with the major population more towards 0.25 to 0.50 mm. Bubbles formed early in the transient could grow to 2 to 3 mm. Bubbles tended to reamin distinct and did not easily coalesce, even when the bubble density was very high.

The flow of nitrogen saturated water can be clearly shown to choke. In fact, it is not even necessary for the water to be saturated. Choking appeared to occur with concentrations as low as 4 percent of saturation. It was possible to vary the back pressure in the nozzle a factor of 10 and not affect the flow rate or pressure profile upstream of the throat. In the converging-diverging nozzle the throat pressure was very low, less than 1 atmosphere. A side result of this was that it was possible to compute the flow rate assuming all water flow through a nozzle with $\Delta P \approx P_o$.

In another nozzle, however, the results were somewhat different. The nozzle was a converging nozzle with an abrupt area change at the "throat," and had glass sidewalls for visual capability. As above, with the water saturated, no gas appeared before the throat of the nozzle and a significant volume of gas appeared downstream in the sudden expansion region. The throat pressure was much higher, about 0.65 MPa. With a nitrogen concentration of only 0.02 cc/g the same flow rate and pressure profile occurred, except that the region downstream of the throat had only a small amount of gas. The throat pressure was slightly different at 0.53 MPa. In both cases, however, this nozzle also acted choked and the flow rate could be computed on the basis of $\Delta P = P_o - P_t$.

Although the flow rates could be computed directly from the ΔP, the throat pressure could not be predicted from some obvious trend in the data. Consequently the flow rates could not be predicted.

REFERENCES

1. Linke, William F.: Solubilities, Inorganic and Metal-Organic Compounds. Vol. II. Fourth ed. Am. Chem. Soc., 1965.

2. Simoneau, R. J.: Pressure Distribution in a Converging-Diverging Nozzle During Two-Phase Choked Flow of Subcooled Nitrogen. Non-Equilibrium Two-Phase Flows, Richard T. Lahey, Jr. and Graham B. Wallis, eds., Am. Soc. Mech. Eng., 1975, pp. 37-45.

3. Cha, Y. S.; and Henry, R. E.: Nitrogen-Water Blowdown Tests. Light-Water-Reactor Safety Research Program. ANL-76-121, Argonne National Laboratory, 1976, pp. 43-47.

4. Cole, R.: Boiling Nucleation. Advances in Heat Transfer, Vol. 10, James P. Hartnett and Thomas F. Irvine, Jr., eds., Academic Press, 1974, pp. 85-166.

5. Holl, J. W.: Nuclei and Cavitation. J. Basic Eng., vol. 92, no. 4, Dec. 1970, pp. 681-688.

6. Ward, C. A.; Balakrishnan, A.; and Hooper, F. C.: On the Thermodynamics of Nucleation in Weak Gas-Liquid Solutions. J. Basic Eng., vol. 92, no. 4, Dec. 1970, pp. 695-704.

7. Epstein, P. S.; and Plesset, M. S.: On the Stability of Gas Bubbles in Liquid-Gas Solutions. J. Chem. Phys., vol. 18, no. 11, Nov. 1950, pp. 1505-1509.

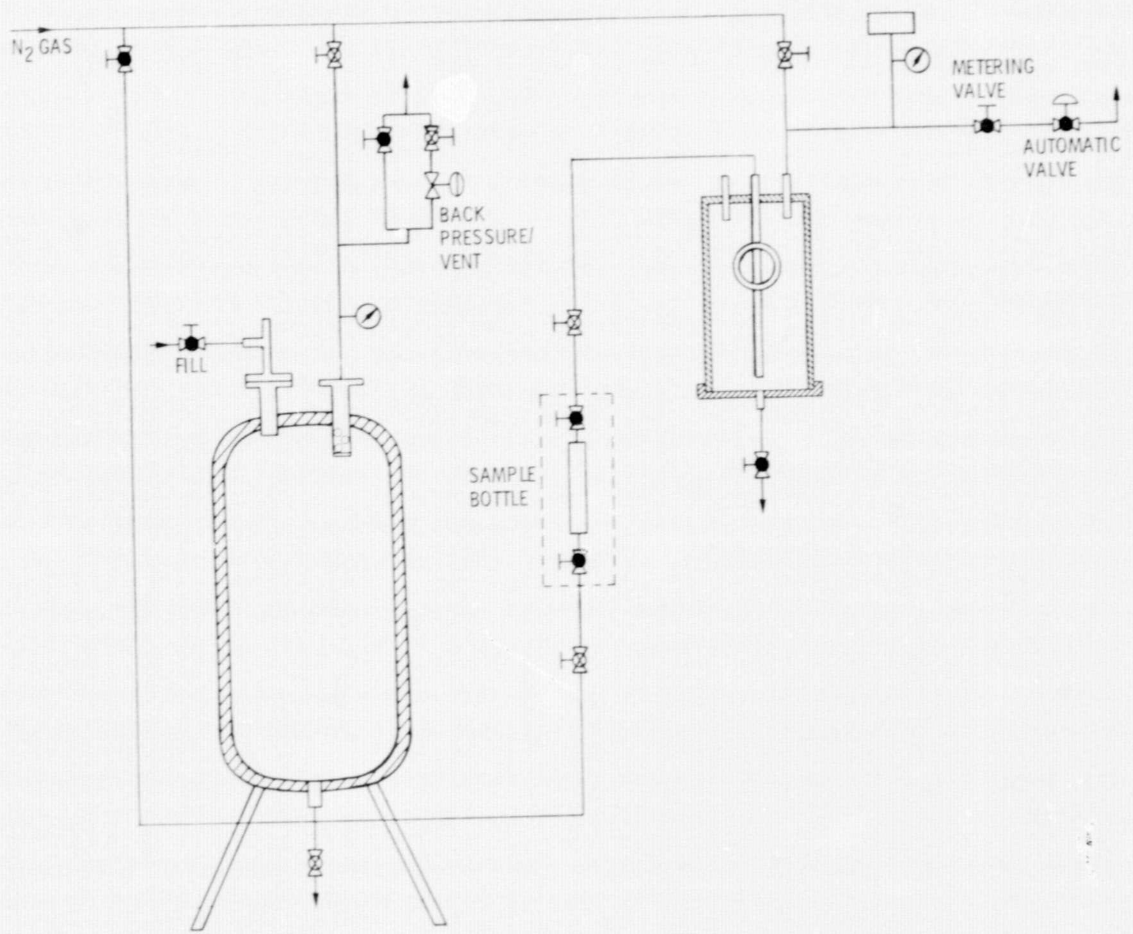

Figure 1. - Static depressurization rig schematic.

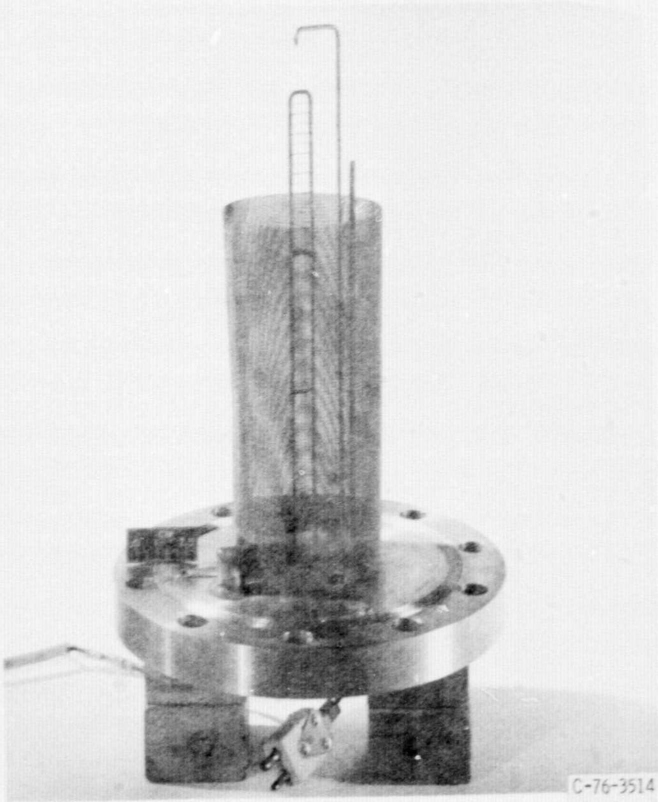

Figure 2. - Static rig internal components.

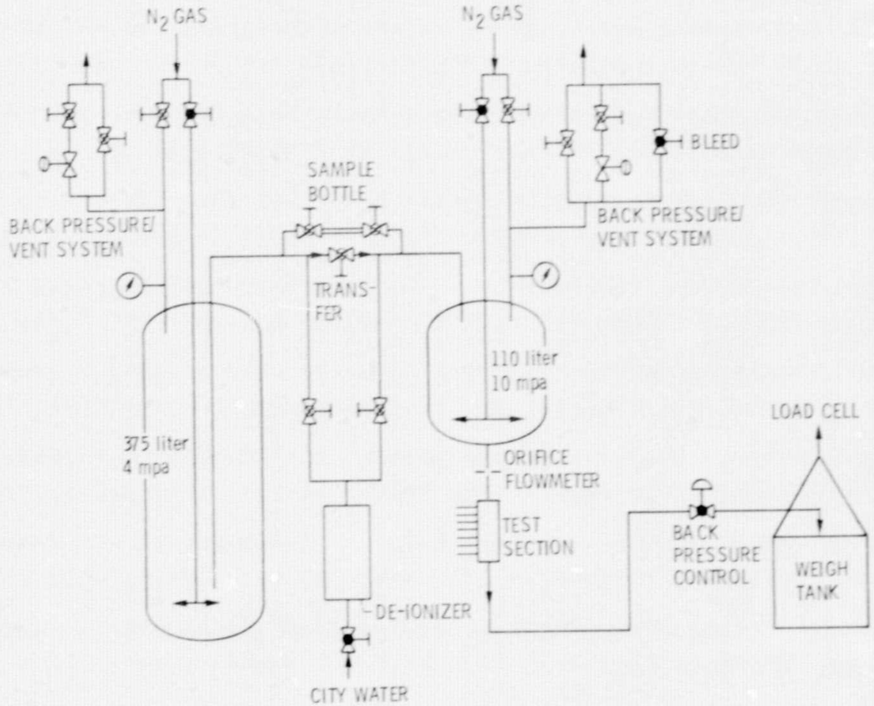

Figure 3. - Flow sytem schematic.

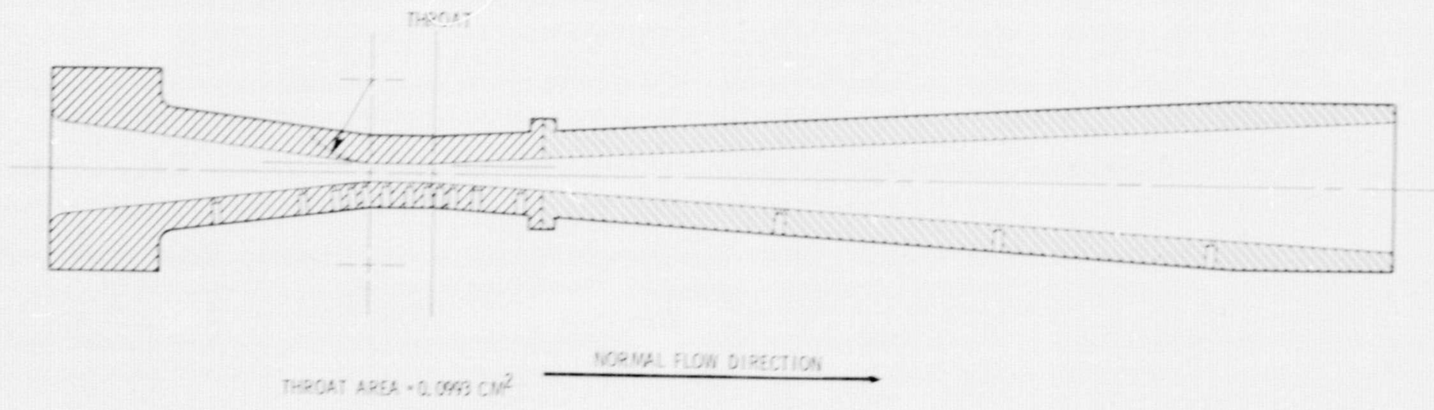

Figure 4. - Axisymmetric converging - diverging nozzle with conical convergence at 7° half angle and divergence at $3\frac{1}{2}$° half angle.

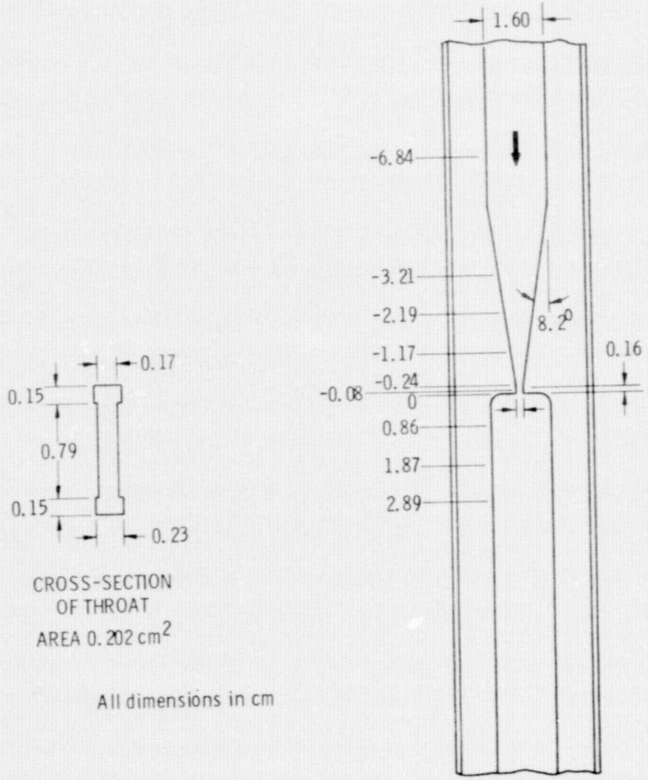

Figure 5. - Flow rig visual test section.

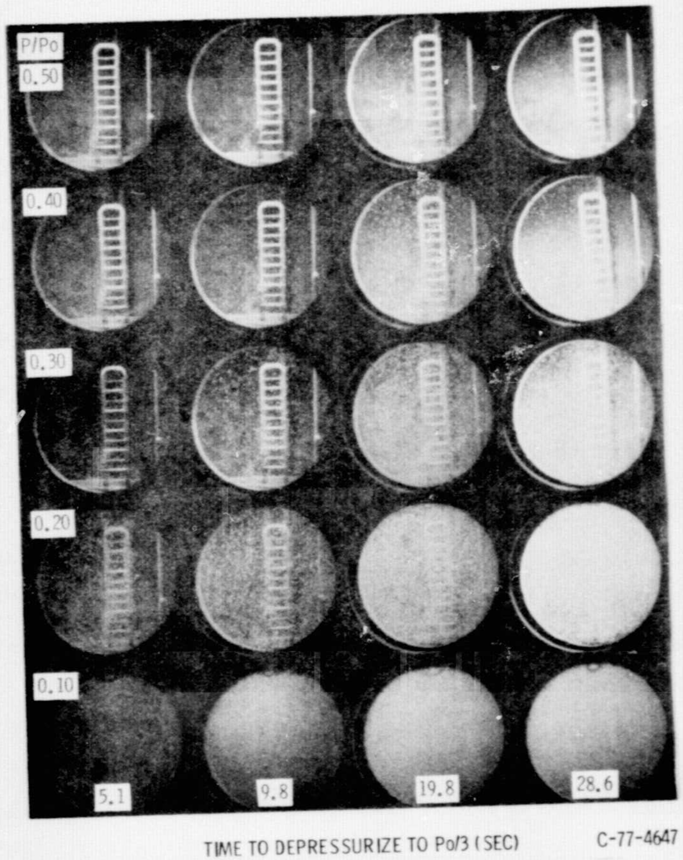

Figure 6. - Influence of depressurization rate on bubble population at various pressure levels. (C_{N_2} = 0.61 cc/gm, saturated.)

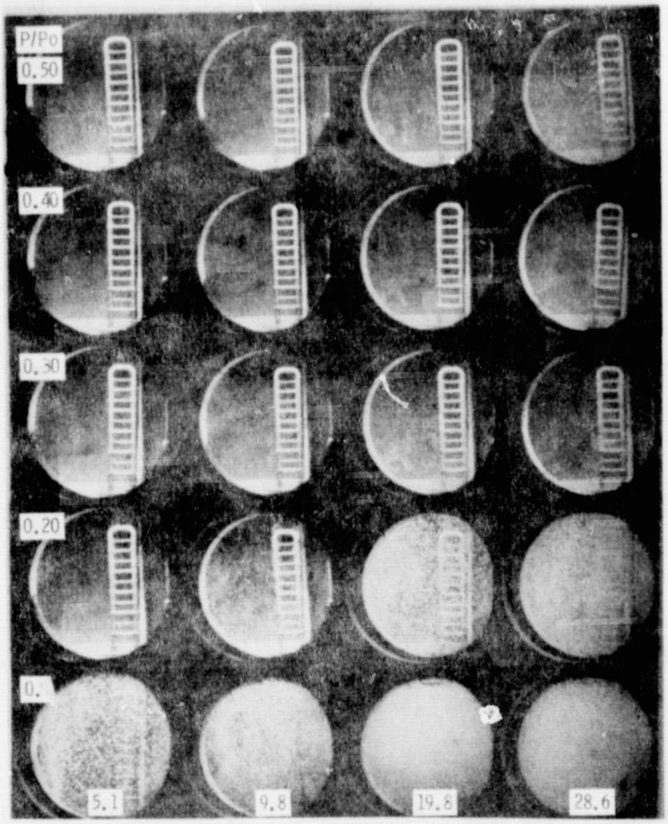

TIME TO DEPRESSURIZE TO Po/3 (SEC) C-77-4648

Figure 7. - Influence of depressurization rate on bubble population at various pressure levels. (C_{N_2} = 0.57 cc/gm.)

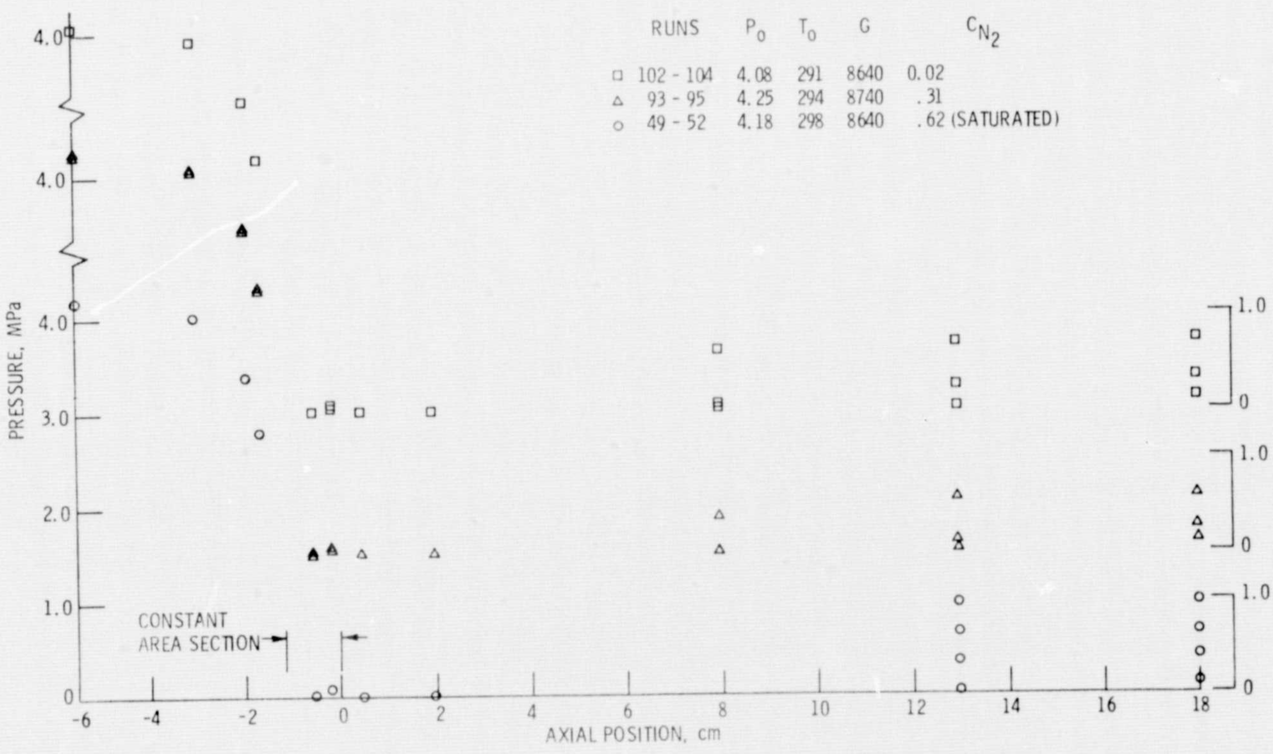

Figure 8. - H_2O/N_2 choked flow. Conical axisymmetric converging-diverging nozzle.

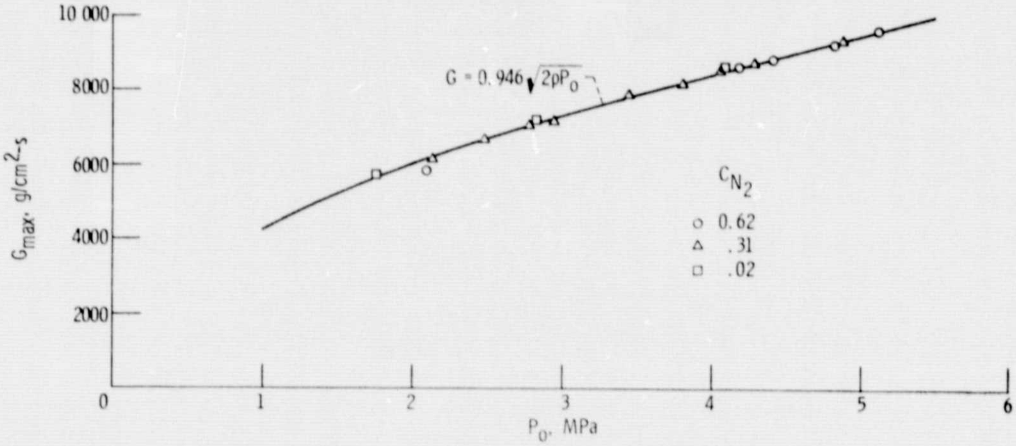

Figure 9. - H_2O/N_2 maximum flow rates. Conical axisymmetric converging-diverging nozzle.

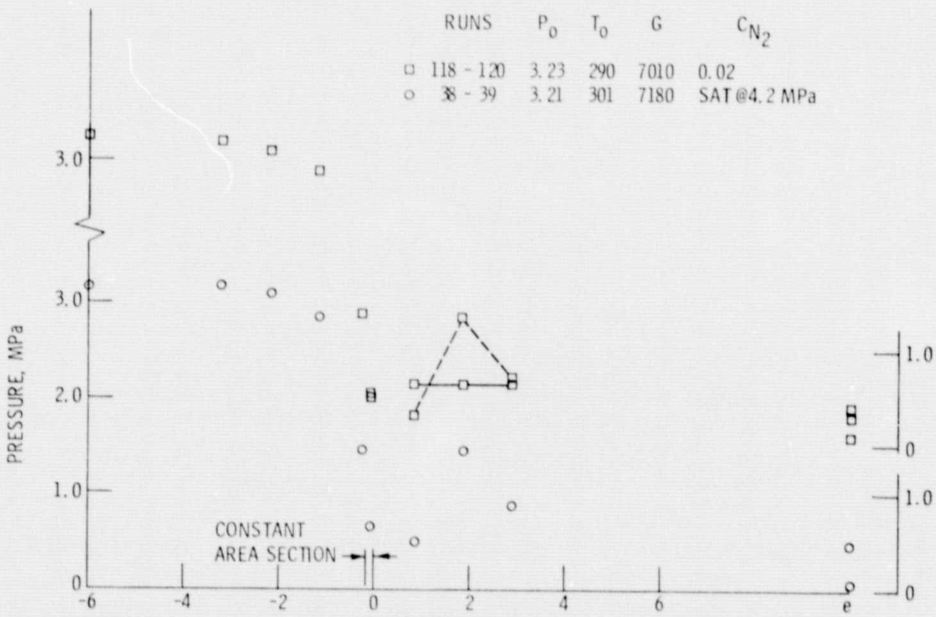

Figure 10. - H_2O/N_2 choked flow. Linear two-dimensional visual converging nozzle.

E-9411-1

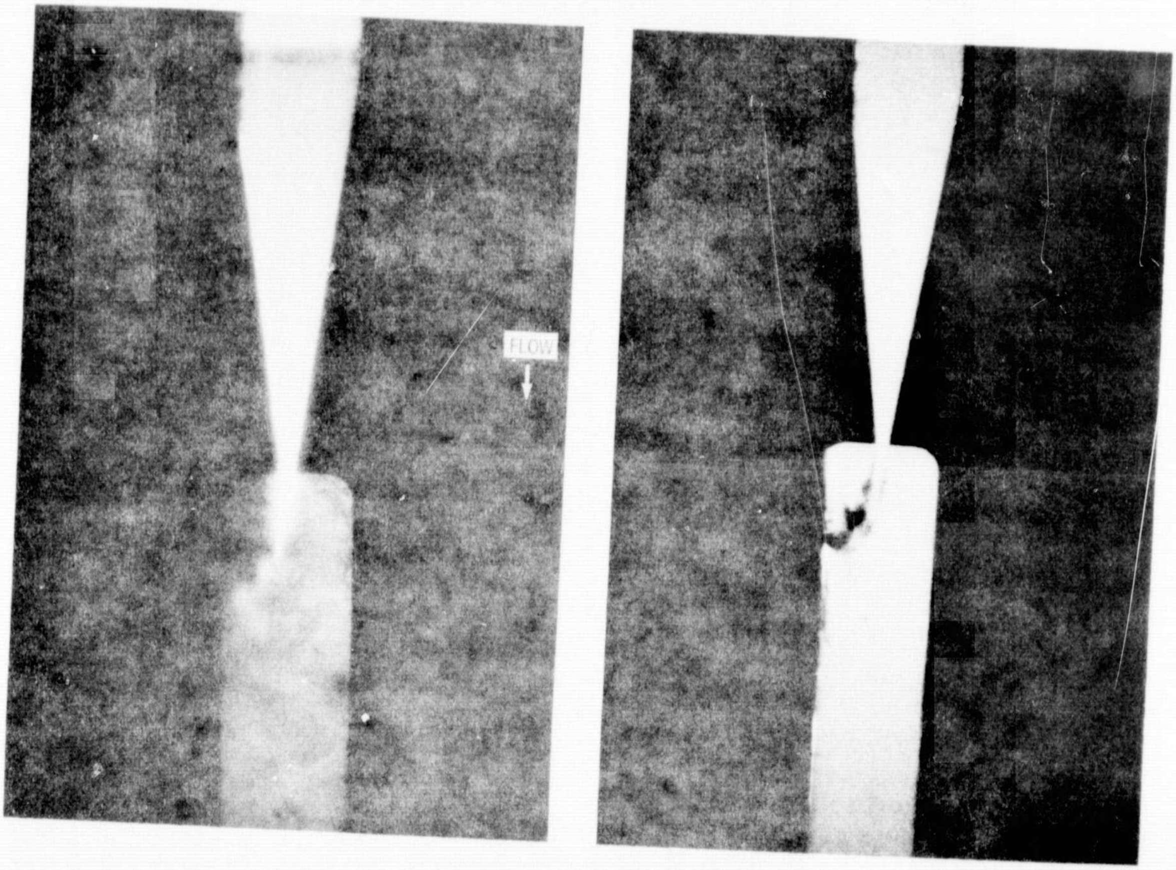

(a) C_{N_2} = 0.62 cc/gm.

(b) C_{N_2} = 0.02 cc/gm.

Figure 11. - Flow of water containing dissolved nitrogen through a converging nozzle.

CS-77-2259